International Journal of Pharmaceutics 415 (2011) 211–217

Contents lists available at ScienceDirect

International Journal of Pharmaceutics

journal homepage: www.elsevier.com/locate/ijpharm

Layer-by-layer microcapsules templated on erythrocyte ghost carriers

Mutukumaraswamy Shaillender[a,1], Rongcong Luo[a,1], Subbu S. Venkatraman[a,*], Björn Neu[b,**]

[a] School of Materials Science and Engineering, Nanyang Technological University, 50 Nanyang Avenue, Singapore 639798, Singapore
[b] School of Chemical and Biomedical Engineering, Nanyang Technological University, Singapore 639798, Singapore

ARTICLE INFO

Article history:
Received 19 April 2011
Accepted 6 June 2011
Available online 14 June 2011

Keywords:
Polyelectrolyte
Layer by layer
Erythrocyte ghost
Microcapsule

ABSTRACT

This work reports the fabrication of layer-by-layer (LbL) microcapsules that provide a simple mean for controlling the burst and subsequent release of bioactive agents. Red blood cell (RBC) ghosts were loaded with fluorescently labeled dextran and lysozyme as model compounds via hypotonic dialysis with an encapsulation efficiency of 27–31%. It is demonstrated that these vesicles maintain their shape and integrity and that a uniform distribution of the encapsulated agents within these carriers is achieved. The loaded vesicles were then successfully coated with the biocompatible polyelectrolytes, poly-L-arginine hydrochloride and dextran sulfate. It is demonstrated that the release profiles of the encapsulated molecules can be regulated over a wide range by adjusting the number of polyelectrolyte layers. In addition, the LbL shell also protects the RBC ghost from decomposition thereby potentially preserving the bioactivity of encapsulated drugs or proteins. These microcapsules, consisting of an RBC ghost coated with a polyelectrolyte multilayer, provide a simple mean for the preparation of loaded LbL microcapsules eliminating the core dissolution and post-loading of bioactive agents, which are required for conventional LbL microcapsules.

1. Introduction

The microencapsulation of substances has been finding many applications in the pharmaceutical, food, cosmetic, paint and print industries (Li et al., 2008; Sokolsky-Papkov et al., 2007). For example, encapsulating pharmaceuticals inside micro-/nano-capsules can help to minimize under- or over-dosing, to protect drugs from degradation, to reduce side-effects, to replace multiple dosing and thus enable better patient compliance (Buket Basmanav et al., 2008; Huang, 2008; Pinto Reis et al., 2006). Various methods including spray-drying, liposome fabrication techniques, interfacial polycondensation and emulsion polymerization have been developed to fabricate micro- and nano-capsules (Caruso et al., 1998; Itou et al., 1999; Wu et al., 2009).

Recently, a simple method to produce microcapsules based on electrostatic attraction and complex formation between anionic and cationic polyelectrolytes has been introduced (Caruso et al., 1998; Neu et al., 2001). By introducing a sacrificial charged template core, anionic and cationic polyelectrolytes are alternately, layer by layer (LbL), deposited onto the template core until the desired numbers of layers have been reached. Subsequently, the core is dissolved and LbL microcapsules are formed (Caruso et al., 1998; Neu et al., 2001). By introducing a sacrificial charged template core, anionic and cationic polyelectrolytes are alternately, layer by layer (LbL), deposited onto the template core until the desired numbers of layers have been reached. Subsequently, the core is dissolved and LbL microcapsules are formed (Gil et al., 2008). Colloidal particles such as melamine formaldehyde, polystyrene latex, or silica seem to be the most extensively used as sacrificial core materials (Peyratout and Dähne, 2004). Though lately drug crystals, protein aggregates, biological cells and carbonate particles including $CaCO_3$, $CdCO_3$ and $MnCO_3$ have also been used (Peyratout and Dähne, 2004).

However, there are some disadvantages in using this method. The template cores need to be removed to produce hollow capsules. This process can be complicated and may lead to rupture of the capsules (Gil et al., 2008). In addition, when dissolving the core, toxic solvents such as hydrofluoric acid, tetrahydrofuran are sometimes required depending on the core material (Shenoy et al., 2003). Toxic residues such as melamine may also be left inside the capsules (Gil et al., 2008). Another problem is the difficulty of incorporating substances inside the capsules, since the loading of substances is done after the formation of the capsules. Consequently, preloaded vesicles could have some advantages as cores for forming LbL microcapsules, which would also eliminate the need to dissolve the core.

One approach recently introduced by Fujimoto and co-workers is to use loaded liposomes as a template core for the LbL deposition (Fujimoto et al., 2007; Fukui and Fujimoto, 2009). Here, we utilize red blood cell (RBC) ghosts as the template core to fabricate LbL

* Corresponding author. Tel.: +65 6790 4259; fax: +65 6790 9081.
** Co-corresponding author. Tel.: +65 9790 6951; fax: +65 6791 1761.
E-mail addresses: assubbu@ntuedu.sg (S.S. Venkatraman), neu@ntu.edu.sg (B. Neu).
[1] Authors contributed equally to this work.

0378-5173/$ – see front matter © 2011 Elsevier B.V. All rights reserved.
doi:10.1016/j.ijpharm.2011.06.011

microcapsules. Due to the biocompatibility and biodegradability of RBC, the application of erythrocyte ghost as biological carriers may provide an interesting alternative to other carrier systems such as liposomes or polymeric particles, as there are no toxic compounds released following carrier degradation. Consequently, several recent works have explored RBC and RBC ghosts as potential carriers for drugs and other bioactive substances (Hamidi and Tajerzadeh, 2003; Hamidi et al., 2007c; Kim et al., 2009).

Various methods to load different kinds of substances into RBC have been developed, such as hypotonic hemolysis, osmotic pulse, chemical perturbation, and electrical breakdown (Hamidi et al., 2001, 2007a, 2007b; Millán et al., 2004). Erythrocyte ghosts were investigated as possible carriers for targeted drug delivery in diseases associated with the mononuclear phagocyte system (Dale et al., 1979; Eichler et al., 1986) and a few studies on targeting them to other cells such as T cells and peritoneal macrophages have been reported (Chiarantini et al., 1995; DeLoach and Droleskey, 1986). However, one of the major problems that still remain is the rapid clearance of erythrocyte ghosts by the mononuclear phagocyte system because of cellular changes occurring during the loading procedure leading to the rapid release of the encapsulated agents (Hamidi et al., 2007b).

In this study, we utilized erythrocyte ghosts as the template core to fabricate LbL microcapsules. These vesicles have several potential advantages as template cores for the preparation of LbL microcapsules such as their uniform shape and high monodispersity. In brief, erythrocyte ghosts were loaded with low molecular mass dextran (3000–5000 Da) and lysozyme (14,700 Da) as model compounds via hypotonic dialysis (Talwar and Jain, 1992a). Due to the soft and fragile nature of erythrocyte ghosts, they were chemically stabilized via glutaraldehyde fixation prior to initiating the LbL adsorption (Neu et al., 2001). These microcapsules were than characterized in terms of morphology, loading efficiency and release behavior.

2. Materials and methods

2.1. Materials

Fluorescein isothiocyanate labeled dextran (FITC-dextran) (3000–5000 Da), poly-L-arginine hydrochloride (PAG) (70,000–130,000 Da), poly-L-lysine hydrobromide (PLL) (30,000–70,000 Da), poly-L-glutamic acid sodium salt (PGA) (50,000–100,000 Da), 25% glutaraldehyde solution, chitosan (medium molecular mass), alginic acid sodium salt (viscosity 20–40 cp), and protamine sulfate (5000–10,000 Da) were purchased from Sigma–Aldrich. Dextran sulfate (DXS) (36,000–50,000 Da) was purchased from MP Biomedicals. All chemicals were used as received. The water used in all experiments was prepared in a Millipore Milli-Q purification system and had a resistivity higher than 18 MΩ cm. Phosphate buffered saline solution (PBS) containing 137 mM sodium chloride, 2.7 mM potassium chloride and 10 mM phosphate buffer was prepared from a 10× PBS stock solution. PBS with different osmolality was prepared from 10× PBS stock solution by adjusting the water volume. The osmolality of solutions was measured using an Advanced Micro Osmometer (Advanced Instruments, Inc. Norwood, MA).

2.2. Preparation of erythrocyte ghosts

Blood samples were withdrawn by venipuncture from healthy volunteers, with informed consent approved according to the procedures of the institutional review board, and transferred to EDTA coated tubes. After centrifugation at 1800 × *g* for 10 min at 4 °C, the plasma and buffy coat was removed and the remaining packed erythrocytes were washed three times with isotonic PBS. 1 ml of packed erythrocytes were washed thrice in 10 ml of 150 mOsm/kg hypotonic PBS via centrifugation at 20,000 × *g* at 4 °C followed by another three washings of the ghost membrane pellet in 10 ml of 100 mOsm/kg hypotonic PBS. The resulting ghost membranes were then dispersed in isotonic PBS and incubated at 37 °C for 1 h to allow the membranes to reseal.

2.3. Loading of erythrocyte ghosts

The erythrocyte ghosts were re-dispersed in 50 mOsm/kg PBS containing FITC-dextran or FITC-lysozyme at the appropriate concentrations and transferred into dialysis bags with 500–1000 Da molecular mass cutoff for FITC dextran and 5000–10,000 Da molecular mass cut off for FITC-lysozyme. The erythrocyte ghosts were then dialyzed against 30 mOsm/kg hypotonic PBS for 2 h at room temperature in order to facilitate loading of the ghosts. Subsequently, the 30 mOsm/kg PBS was changed to isotonic PBS and dialyzed for another 2 h at 37 °C to reseal the erythrocyte ghosts. Thereafter the loaded vesicles were washed 4 times with isotonic PBS to separate them from free, un-encapsulated macromolecules.

2.4. Polymer coating of erythrocyte ghosts

Prior to the LbL adsorption, the loaded erythrocyte ghosts were fixed with 2.5% glutaraldehyde solution for 1 h at 4 °C. For the LbL adsorption, the fixed vesicles were added to a solution containing 0.5 mg/ml of the respective polyelectrolyte in 0.1 M NaCl. After incubating the vesicles with the polymer solution for 10 min at room temperature, they were washed twice in isotonic PBS to remove non-adsorbed polyelectrolytes before coating the vesicles with the next polyelectrolyte layer. LbL consecutive adsorption of positive and negative charged polyelectrolytes was carried out by repeating these steps in sequence until the desired layer number was achieved.

2.5. Characterization of LbL-microcapsules

In order to quantitatively study the amounts of FITC-dextran loaded into the bare RBC ghosts, aliquots of the loaded vesicles were dispensed into 1.5 ml Eppendorf tubes and 1% Triton X-100 was added to completely lyse the loaded erythrocyte ghosts. The supernatant was placed into black 96-microwell plates and the intensity of each well was read at an excitation and emission wavelength of 485 and 535 nm, respectively, using a UV spectrofluorophotometer microplate reader (Perkin Elmer Victor 1420, USA).

2.6. Microscopic techniques

A confocal laser scanning microscope (CLSM) (Zeiss LSM 510) was used to study the distribution of FITC-dextran in the loaded vesicles. Scanning electron microscopy (SEM) (JSM-5310, Jeol Ltd) was employed to study and compare morphological differences between RBC and RBC ghosts. Standard procedures for preparing the samples for SEM were employed. In brief, one drop of the sample suspension was put onto a clean silicon wafer and dried at 37 °C and coated with a fine gold film and observed under a 5 kV accelerating voltage.

2.7. Electrophoretic mobility measurements

In order to monitor the layering process, the electrophoretic mobilities of the bare and coated vesicles were measured using a Malvern Zetasizer (Malvern Zetasizer Nano, UK). The elec-

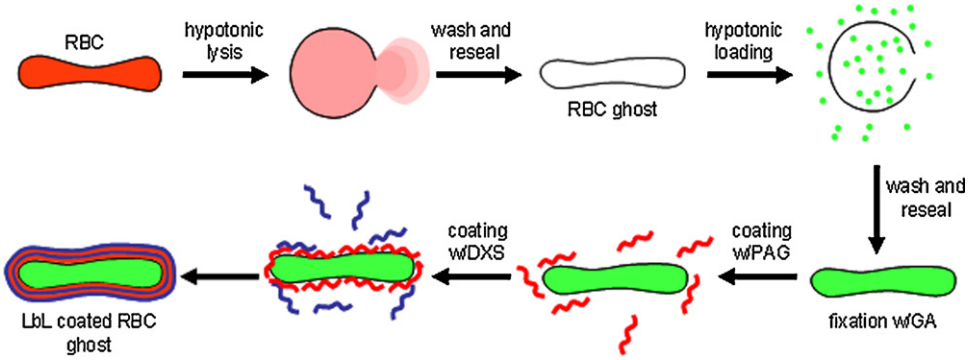

Fig. 1. Schematic illustration of the preparation of layer-by-layer microcapsules with erythrocyte ghosts as templates.

trophoretic mobility was converted into the respective ζ-potentials using the Smoluchowski relationship.

2.8. Release of macromolecules from LbL-microcapsules

The release of FITC-dextran and FITC-lysozyme was studied and compared between bare and coated RBC ghosts. For this purpose, equal amounts of coated and uncoated erythrocyte ghost were added to 500 μl PBS and kept at 37 °C. At defined time intervals, the samples were centrifuged and 500 μl of supernatant was collected to analyze for the fluorescence intensity and the ghosts were resuspended in 500 μl of fresh isotonic PBS.

3. Results and discussion

3.1. Preparation of erythrocyte ghosts

In order to prepare erythrocyte ghosts, erythrocytes are initially suspended in hypotonic PBS of 150 mOsm/kg (Fig. 1). Due to the osmotic imbalance, the erythrocytes begin to swell and pores open up in the membrane allowing hemoglobin to leach out. Thereafter erythrocytes are suspended in hypotonic PBS of 100 mOsm/kg to allow any remaining hemoglobin to leach out. Lastly, the erythrocyte membranes are resealed in isotonic PBS to obtain erythrocyte ghosts.

Fig. 2 shows scanning electron microscopy (SEM) images of erythrocytes (a) and ghosts (b and c). The original erythrocytes show the typical discoidal shape and have a flat surface (Fig. 2a). In contrast, ghost vesicles appear flat with several folds and creases on the surface (Fig. 2b and c). In order to investigate the effects of the osmolality on the vesicle shape, erythrocytes were also suspended in hypotonic PBS having a much lower osmolality of 20 mOsm/kg followed by resealing in isotonic PBS. As shown in Fig. 2d, most of these ghost vesicles cannot retain their shape and integrity. It can thus be concluded that when the osmolality is reduced below a certain limit, irreversible ruptures and openings of the membrane will occur.

3.2. Preparation of loaded erythrocyte ghosts

FITC-dextran and FITC-lysozyme were loaded into erythrocyte ghosts as model compounds via hypotonic dialysis as schematically illustrated in Fig. 1. SEM images of the loaded vesicles show that these RBC ghost carriers still resemble the original shape (Fig. 3) indicating that the loading procedure does not induce morphological changes. To visualize the distribution of FITC-dextran in the RBC ghosts, confocal laser scanning microcopy (CLSM) pictures of the loaded carriers were taken in several planes separated by 0.5 μm. As can be seen in Fig. 4, these vesicles are completely and uniformly filled confirming the encapsulation of these macromolecules.

Table 1 summarizes the encapsulation efficiency (EE) and the loaded amounts (LA) with the encapsulation efficiency denoting the percentage ratio of the loaded FITC-dextran relative to the initially added amount, whereas the loaded amount corresponds to the total amount of FITC-dextran encapsulated. The encapsulation efficiency shows only small variations independent on the initial feed amounts of 28–31%. Consequently, the loaded amounts increase steadily with increasing feed amounts (Table 1). It should be noted that the encapsulation efficiency is in the same range as reported in other studies where RBC ghosts were used to encapsulate various agents such as drugs, enzymes, peptides, proteins, polysaccharides and DNA (Hamidi et al., 2001, 2007b; Millán et al., 2004).

3.3. Polymer coating of RBC ghosts

Considering the potential biomedical applications of LbL microcapsules, different biopolymers including polypeptides and polysaccharides were tested for their suitability as shell materials. The polyelectrolyte pairs tested in this study included chitosan/alginate, protamine sulfate/DXS, PLL/PGA, PLL/DXS and PAG/DXS since these polymers are widely regarded as biocompatible and biodegradable (Gil et al., 2008; Peyratout and Dähne, 2004). Initially, aggregation of loaded ghosts after coating with each polyelectrolyte combination was investigated via optical microscopy. Since PAG/DXS demonstrated the least aggregation, it was used throughout this study. It should be noted that RBC ghosts are rather soft and fragile, thus to avoid breakage of these vesicles due coagulation and aggregation during the LbL deposition of polyelectrolytes they were stabilized via glutaraldehyde fixation prior to the polyelectrolyte coating and gently resuspended and centrifuged after each coating step.

To monitor the polyelectrolyte layering process the ζ-potential was recorded after each coating step. As shown in Fig. 5, RBC ghosts have a negative ζ-potential of −50 mV, which changes to a positive value (+38 mV) after the deposition of the first cationic polyelectrolyte layer (PAG). This indicates that the surface charge of the RBC ghosts is overcompensated by the PAG molecules. The charge overcompensation resulting from PAG facilitates the subsequent deposition of the anionic polyelectrolyte layer (DXS). From Fig. 5, a net reversal of surface charge between positive and negative values

Table 1
Encapsulation efficiency (EE) and loading amounts (LA) of FITC-dextran into RBC ghosts.

Initial feeding (μg)	EE (%)	LA (pg/cell)
200	27.9 ± 1.6	12.1
400	30.9 ± 2.3	22.4
600	31.1 ± 0.4	39.1

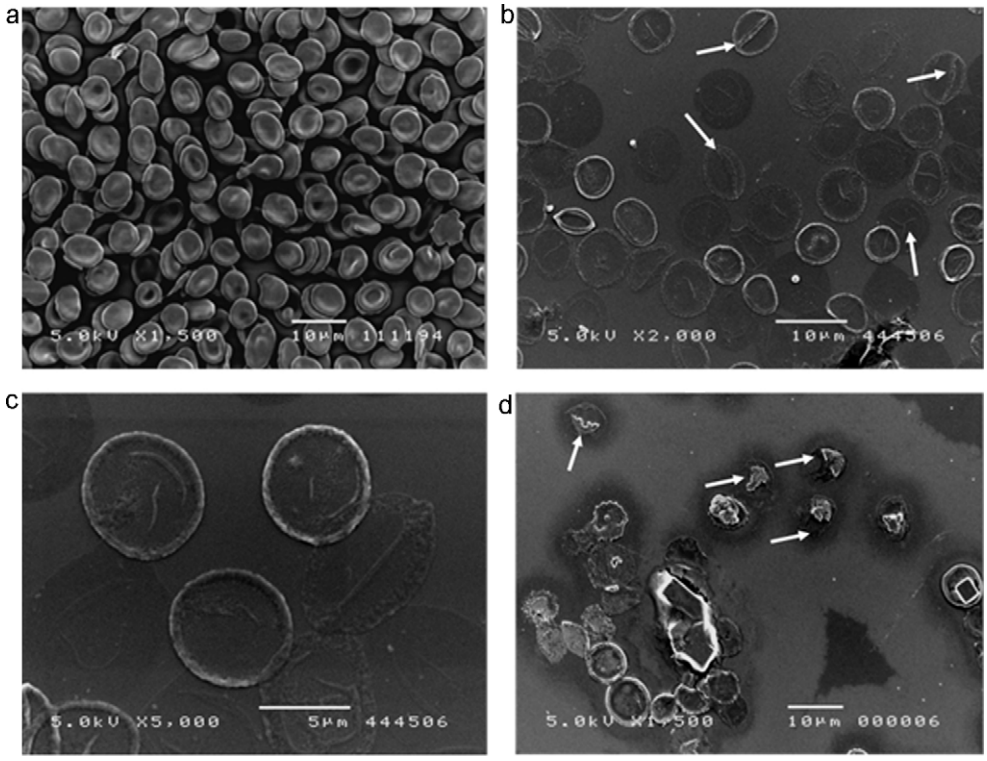

Fig. 2. Morphology of RBC and RBC ghosts. Scanning electron microcopy image of (a) RBC, (b) well resealed RBC ghosts, (c) enlarged view of well resealed RBC ghosts, and (d) poorly resealed RBC ghosts.

is evident for each polyelectrolyte layer, suggesting the successful coating of the RBC ghosts.

To quantify the amount of the loaded dextran or lysozyme released during the layering procedure, the amounts in the supernatant after each coating step were quantified. Fig. 6 shows the relative amount of these macromolecules left inside the capsules after layering, with 100% denoting the amount present in the ghosts before fixation with glutaraldehyde. It should be noted that the amount lost during the layering is significantly larger for dextran as compared to lysozyme. The remaining FITC-dextran was in the range of 35–39%, whereas for lysozyme it was around 66–75%. It seems likely that this can be attributed, at least partly, to the size of these molecules. Dextran is smaller and it can thus be expected to diffuse more rapidly through the polyelectrolyte layers.

3.4. Release behaviors of LbL microcapsules

The next step was to study the release profiles of the encapsulated model compounds. Fig. 7a shows the FITC-dextran release from bare RBC ghosts and LbL-coated RBC ghosts. Within the initial 2 h, approximately 40% of the FITC-dextran is released from the uncoated ghosts followed by a significant reduction of the release rate, with about another 43% of the FITC dextran being released within the next 300 h. This release behavior is very similar to that of other nano- or microparticle delivery systems based on polymeric matrices, where a burst release is usually followed by a slower release (Pinto Reis et al., 2006). In many cases, the burst release is undesirable, as it may lead to toxicity or wastage of the encapsulated agent.

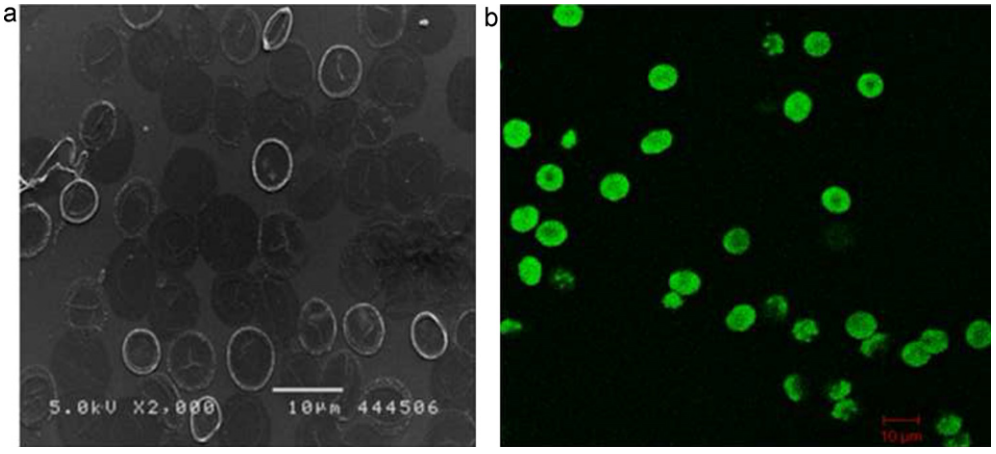

Fig. 3. RBC ghosts loaded with FITC labeled dextran. (a) Scanning electron microcopy image illustrating the morphology of the ghost carriers and (b) confocal laser scanning microcopy image showing the distribution of the labeled dextran within the RBC ghost.

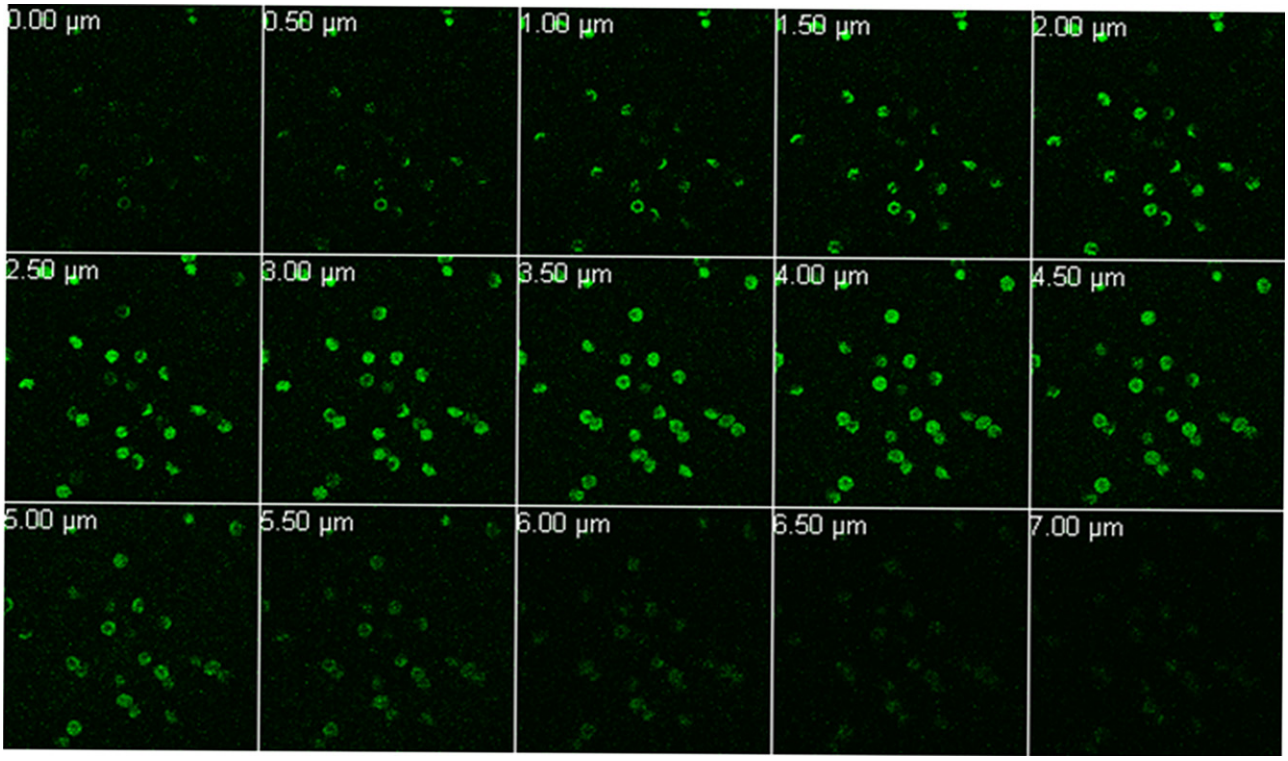

Fig. 4. Confocal microscopy images of RBC ghosts loaded with FITC labeled dextran. The scans were made in 15 planes separated by a distance of 0.5 µm.

In contrast, the LbL coating of the RBC ghosts suppresses the initial burst release of FITC-dextran even with only three polyelectrolyte layers as shown in Fig. 7a. Since the FITC-dextran release was determined in the same buffer as used for the polyelectrolyte deposition, it can be concluded that a tight polyelectrolyte complex between PAG and DXS is formed that blocks the FITC-dextran release, although it has already been released from the interior of the core. Due to this retardation, which is primarily a partitioning effect coupled to diffusion, only about 39% of the FITC-dextran has been released after ~290 h from the vesicles coated with three polyelectrolyte layers. For 5, 7 and 9 layer-coated vesicles, the FITC-dextran release is further reduced to 30%, 25% and 21% during the same interval (Fig. 7a). This in vitro release behavior demonstrates that controlled release can be achieved simply by adjusting the layer numbers.

To confirm the trends observed for the dextran release from LbL coated capsules, we also incorporated FITC labeled lysozyme into RBC ghosts. The release profiles are plotted in Fig. 7b. Similar to FITC-dextran, lysozyme also shows a burst release of around 40% from bare vesicles within the first 2 h. This release is reduced significantly to 20% after coating the vesicles with three polyelectrolyte layers (Fig. 7b). The subsequent release of lysozyme also decreases with increasing layer numbers, similar to the trend observed for FITC-dextran (Fig. 7a). Within ~290 h, about 86% of the lysozyme has been released from bare RBC ghosts whereas the release of ghosts coated with nine polyelectrolyte layers is reduced to 39%. It should be emphasized that the release profile of lysozyme is significantly different from that of dextran. This could be attributed to differences in the nature and size of these macromolecules.

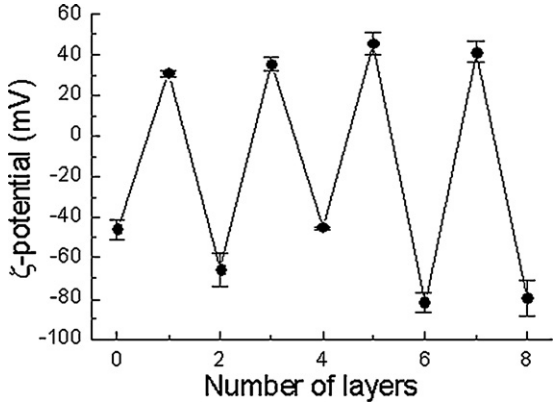

Fig. 5. ζ-Potential of RBC ghosts as a function of the number of polyelectrolyte layers. Loaded RBC ghosts were fixed with glutaraldehyde and coated with PAG and DXS.

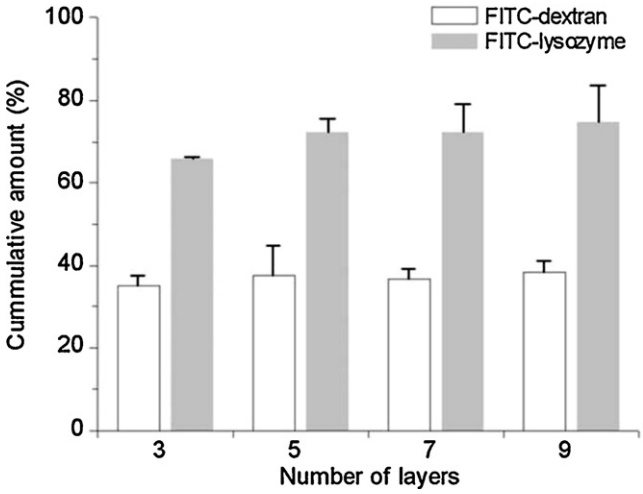

Fig. 6. Mean amount of FITC-dextran and FITC-lysozyme present in loaded RBC ghosts after the LbL coating with different numbers. 100% refers to the amount present in the vesicles before initiating the coating procedure with the polyelectrolytes.

Table 2
Release parameters of FITC-dextran and FITC-lysozyme.

Number of layers	Burst duration (h)[a]	Burst release (%)[b]		Release rate (ng/h)[c]		*n*-Value[d]	
		Dextran	Lysozyme	Dextran	Lysozyme	Dextran	Lysozyme
0	28.5	66.3	75.8	7.0 ± 0.21	3.6 ± 0.13	0.26	0.09
3	33	22.7	47.3	2.0 ± 0.12	5.0 ± 0.62	0.33	0.23
5	32	15.6	45.2	1.9 ± 0.06	4.6 ± 0.24	0.35	0.22
7	30	11.5	29.3	2.0 ± 0.08	5.1 ± 0.88	0.44	0.28
9	29.5	9.6	20.1	1.8 ± 0.08	4.3 ± 0.72	0.42	0.25

[a] Time point where the initial burst release ends estimated from Fig. 7.
[b] Amount released during the initial burst release.
[c] Release rate following the initial burst release.
[d] *n*-Value from a power law fit ($y = kt^n$) of the release profile following the initial burst release.

Nevertheless, these results clearly indicate that the concept of polyelectrolyte-encapsulated vesicles should allow controlling the release of a wide range of bioactive molecules.

The release profiles also reveal that the polyelectrolyte layers prevent or reduce the initial burst release. For both dextran and lysozyme, the addition of polyelectrolyte layers suppresses the burst significantly (Table 2). With nine layers, the burst is reduced to about 11% (~6×) for dextran and about 20% (~3.5×) for lysozyme. The difference in the extent of the suppression of the burst might be attributed to a greater partitioning of lysozyme into the polyelectrolyte layers as compared to dextran, hence making it more difficult to suppress its burst.

In addition to reducing the burst release, it is also desirable that a drug carrier maintains a slower, controlled release rate following the initial burst release. The release kinetics of the encapsulated substances were analyzed over the region following the burst release as shown in Table 2. In case of FITC-dextran, the release rate of bare RBC ghosts is approximately 3.5 times higher as compared to vesicles with three polyelectrolyte layers. For lysozyme, a comparable reduction of the initial burst release is only achieved with seven or nine polyelectrolyte layers. The subsequent release rates are hardly affected by the number of polyelectrolyte layers. The difference in the extent of the suppression might be due to the lower molar mass of the encapsulated dextran or due to partitioning effects.

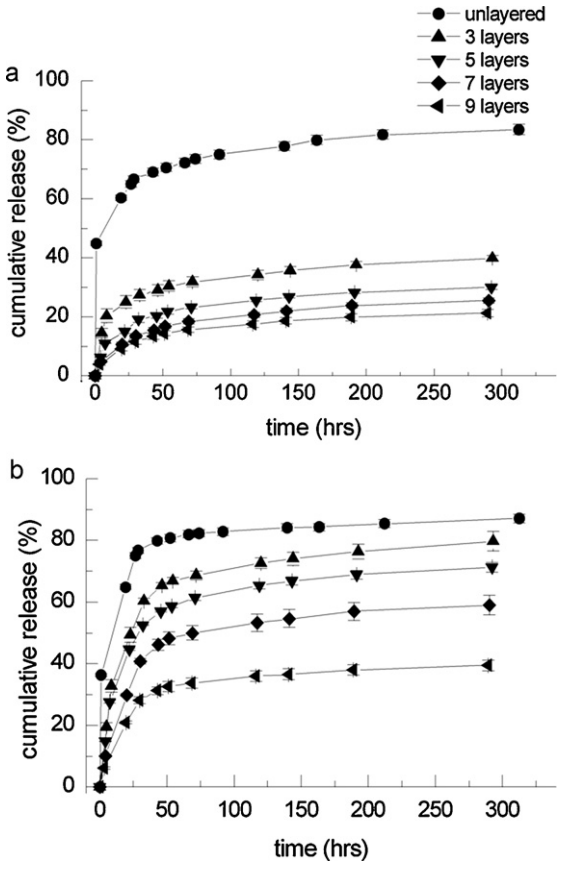

Fig. 7. Release profiles of (a) FITC-dextran and (b) FITC-lysozyme from RBC ghosts as a function of the time and number of polyelectrolyte layers.

The kinetics of the drug release from erythrocyte carriers depends on the size and polarity of the encapsulated agents. In general three different patterns of drug release can be observed: (1) the drug release occurs by rapid diffusion through the membrane for lipophilic drugs such as primaquin (Talwar and Jain, 1992a), methotrexate (Lewis and Alpar, 1984), (2) the drug release occurs by cell lysis for polar drugs such as enalaprilat (Hamidi et al., 2001) or gentamicin (Eichler et al., 1986), and (3) the release profile is intermediate between the first two patterns, as observed for erythropoietin (Garín et al., 1996) and isoniazid (Jain et al., 1995). Among the different strategies to control the release of drugs from erythrocytes, crosslinking with glutaraldehyde seems to be one of the most successful to date (Talwar and Jain, 1992b). This study demonstrates a new method for controlling the release of low and high molar mass bioactives from erythrocyte carriers by varying the shell thickness, independent of the nature of the macromolecules. By suitable choice of the number and type of polyelectrolyte layers, it is possible to fine-tune the entire release curve, without depending on lysis of these carriers to control the release.

Lastly, the shell resistance to surfactant treatment was investigated by exposing the bare RBC ghosts and LbL microcapsules to Triton X-100. 100% FITC-dextran release is observed after the treatment of uncoated ghosts, indicating complete membrane lysis. However, for ghosts coated with 3, 5, 7 and 9 polyelectrolyte layers, this treatment cannot induce a complete release of the FITC dextran from the microcapsules, suggesting that the deposited polyelectrolyte layers can effectively resist penetration of Triton X-100 and thus protect the core from decomposition. This is an important feature in that it demonstrates that this method also helps to preserve the bioactivity of the encapsulated drugs or proteins, besides ensuring that the release is controlled and solely governed by diffusion.

4. Conclusion

This study employed pre-loaded RBC ghosts as template cores for the fabrication of polyelectrolyte multilayer capsules via LbL deposition, simplifying the preparation of loaded LbL microcapsules. Different layers of PAG and DXS were deposited successfully onto negatively charged RBC ghosts. These polyelectrolyte multilayers successfully suppressed the burst and subsequent release of FITC-dextran. To a lower extent, the layered carriers also reduced the burst of lysozyme. Besides controlling the release rate, these carriers also offer the possibility to protect the bioactive agents from the external environment. In conclusion, these novel LbL

microcapsules have several unique properties such as ease of preparation, tunable release, biocompatibility, biodegradability, and the possibility of multi-functionality. The concept of erythrocyte ghost carriers coupled with polyelectrolyte multilayers is therefore a promising alternative to other carrier systems and should be further explored for suitable drug delivery applications.

Acknowledgements

This work was supported by grants from the Ministry of Education (Singapore) and the National Research Foundation (Singapore).

References

Buket Basmanav, F., Kose, G.T., Hasirci, V., 2008. Sequential growth factor delivery from complexed microspheres for bone tissue engineering. Biomaterials 29, 4195–4204.

Caruso, F., Caruso, R.A., Möhwald, H., 1998. Nanoengineering of inorganic and hybrid hollow spheres by colloidal templating. Science 282, 1111–1114.

Chiarantini, L., Rossi, L., Fraternale, A., Magnani, M., 1995. Modulated red blood cell survival by membrane protein clustering. Mol. Cell. Biochem. 144, 53–59.

Dale, G.L, Kuhl, W., Beutler, E., 1979. Incorporation of glucocerebrosidase into Gaucher's disease monocytes in vitro. Proc. Natl. Acad. Sci. U.S.A. 76, 473–475.

DeLoach, J.R., Droleskey, R., 1986. Survival of murine carrier erythrocytes injected via peritoneum. Comp. Biochem. Physiol. A 84, 447–450.

Eichler, H.G., Gasic, S., Bauer, K., 1986. In vivo clearance of antibody-sensitized human drug carrier erythrocytes. Clin. Pharmacol. Ther. 40, 300–303.

Fujimoto, K., Toyoda, T., Fukui, Y., 2007. Preparation of bionanocapsules by the layer-by-layer deposition of polypeptides onto a liposome. Macromolecules 40, 5122–5128.

Fukui, Y., Fujimoto, K., 2009. The preparation of sugar polymer-coated nanocapsules by the layer-by-layer deposition on the liposome. Langmuir 25, 10020–10025.

Garín, M.I., López, R.M., Sanz, S., Pinilla, M., Luque, J., 1996. Erythrocytes as carriers for recombinant human erythropoietin. Pharm. Res. 13, 869–874.

Gil, P.R., del Mercato, L.L., del Pino, P., Muñoz-Javier, A., Parak, W.J., 2008. Nanoparticle-modified polyelectrolyte capsules. Nano Today 3, 12–21.

Hamidi, M., Tajerzadeh, H., 2003. Carrier erythrocytes: an overview. Drug Deliv.: J. Deliv. Target. Ther. Agents 10, 9–20.

Hamidi, M., Tajerzadeh, H., Dehpour, A.R., Rouini, M.R., Ejtemaee-Mehr, S., 2001. In vitro characterization of human intact erythrocytes loaded by enalaprilat. Drug Deliv.: J. Deliv. Target. Ther. Agents 8, 223–230.

Hamidi, M., Zarei, N., Zarrin, A.H., Mohammadi-Samani, S., 2007a. Preparation and in vitro characterization of carrier erythrocytes for vaccine delivery. Int. J. Pharm. 338, 70–78.

Hamidi, M., Zarrin, A., Foroozesh, M., Mohammadi-Samani, S., 2007b. Applications of carrier erythrocytes in delivery of biopharmaceuticals. J. Control. Release 118, 145–160.

Hamidi, M., Zarrin, A.H., Foroozesh, M., Zarei, N., Mohammadi-Samani, S., 2007c. Preparation and in vitro evaluation of carrier erythrocytes for RES-targeted delivery of interferon-alpha 2b. Int. J. Pharm. 341, 125–133.

Huang, S.L., 2008. Liposomes in ultrasonic drug and gene delivery. Adv. Drug Deliv. Rev. 60, 1167–1176.

Itou, N., Masukawa, T., Ozaki, I., Hattori, M., Kasai, K., 1999. Cross-linked hollow polymer particles by emulsion polymerization. Colloids Surf., A 153, 311–316.

Jain, S, Jain, S.K., Dixit, V.K., 1995. Erythrocytes based delivery of isoniazid: preparation and in-vitro characterization. Indian Drugs 32, 471–476.

Kim, S.H., Kim, E.J., Hou, J.H., Kim, J.M., Choi, H.G., Shim, C.K., Oh, Y.K., 2009. Opsonized erythrocyte ghosts for liver-targeted delivery of antisense oligodeoxynucleotides. Biomaterials 30, 959–967.

Lewis, D.A., Alpar, H.O., 1984. Therapeutic possibilities of drugs encapsulated in erythrocytes. Int. J. Pharm. 22, 137–146.

Li, M., Rouaud, O., Poncelet, D., 2008. Microencapsulation by solvent evaporation: state of the art for process engineering approaches. Int. J. Pharm. 363, 26–39.

Millán, C.G., Marinero, M.L.S., Castañeda, A.Z., Lanao, J.M., 2004. Drug, enzyme and peptide delivery using erythrocytes as carriers. J. Control. Release 95, 27–49.

Neu, B, Voigt, A., Mitlöhner, R., Leporatti, S., Gao, C.Y., Donath, E., Kiesewetter, H., Möhwald, H., Meiselman, H.J., Bäumler, H., 2001. Biological cell as templates for hollow microcapsules. J. Microencapsulation 18, 385–395.

Peyratout, C.S., Dähne, L., 2004. Tailor-made polyelectrolyte microcapsules: from multilayers to smart containers. Angew. Chem. Int. Ed. 43, 3762–3783.

Pinto Reis, C., Neufeld, R.J., Ribeiro, A.J., Veiga, F., 2006. Nanoencapsulation. I. Methods for preparation of drug-loaded polymeric nanoparticles. Nanomed.: Nanotechnol. Biol. Med. 2, 8–21.

Shenoy, D.B., Antipov, A.A., Sukhorukov, G.B., Möhwald, H., 2003. Layer-by-layer engineering of biocompatible, decomposable core-shell structures. Biomacromolecules 4, 265–272.

Sokolsky-Papkov, M., Agashi, K., Olaye, A., Shakesheff, K., Domb, A.J., 2007. Polymer carriers for drug delivery in tissue engineering. Adv. Drug Deliv. Rev. 59, 187–206.

Talwar, N., Jain, N.K., 1992a. Erythrocyte based delivery system of primaquine: in vitro characterization. J. Microencapsulation 9, 357–364.

Talwar, N., Jain, N.K., 1992b. Erythrocytes as carriers of metronidazole: in-vitro characterization. Drug Dev. Ind. Pharm. 18, 1799–1812.

Wu, Y., Mackay, J.A., McDaniel, J.R., Chilkoti, A., Clark, R.L., 2009. Fabrication of elastin-like polypeptide nanoparticles for drug delivery by electrospraying. Biomacromolecules 10, 19–24.